Integral Equation Theory of Adsorption in Templated Materials: Influence of Molecular Attraction†

ARTICLE *in* THE JOURNAL OF PHYSICAL CHEMISTRY C · OCTOBER 2007

Impact Factor: 4.77 · DOI: 10.1021/jp073536g

2 AUTHORS, INCLUDING:

Lev Sarkisov
The University of Edinburgh
60 PUBLICATIONS **1,629** CITATIONS

SEE PROFILE

Integral Equation Theory of Adsorption in Templated Materials: Influence of Molecular Attraction†

Lev Sarkisov*,‡ and Paul R. Van Tassel§

Institute for Materials and Processes, University of Edinburgh, Edinburgh, EH9 3JL, United Kingdom, and Department of Chemical Engineering, Yale University, New Haven, Connecticut 06520-8286

Received: May 9, 2007; In Final Form: August 13, 2007

Understanding the fundamental properties of fluids under confinement in templated porous media is important for the rational design of materials with tailored functions. However, theoretical descriptions remain elusive. Although a number of approaches have been developed within the replica Ornstein−Zernike (ROZ) formalism, they have thus far been limited mainly to simple species. Another challenge is associated with the general applicability of integral equation theories, originally developed for bulk liquids, to confined systems in general and, in particular, to molecular systems confined in templated structures. In this work, we extend our previous theory of molecular species adsorbed in a templated porous material (a ROZ solution to a reference interaction site model) to systems with attractive interactions. We explore the scope and applicability of direct routes toward the chemical potential in combination with several well-established closures, such as Percus−Yevick, mean spherical approximation, hypernetted chain closure (HNC), partially linearized HNC (PLHNC), and Martynov−Sarkisov. The relative accuracy, thermodynamic consistency, and ease of convergence are explored. Although only semiquantitative agreement can be expected from these approximate closure relations, we demonstrate that the proposed theory predicts templated molecular recognition with reasonable accuracy.

1. Introduction

Molecular templating is a simple and versatile technique to create functional materials for a number of applications.[1] The idea of templating is simple. The initial reaction mixture involves precursor monomers and template molecules. This is followed by polymerization and template species removal. The cavities left in the structure are energetically and sterically complementary to the template molecules. (Often a lock-and-key analogy is used to explain this effect.) Materials prepared in this fashion can in principle recognize and bind molecules or supramolecular groups identical or similar to the original template. This biomimetic molecular recognition functionality can be exploited in separations, sensing, enzyme immobilization, and other applications.[2−4]

A particularly successful implementation of this idea is associated with molecularly imprinted polymers (MIP). For example, one of the earliest MIP was prepared using methacrylic acid (MAA) as the functional monomer and ethylene glycol dimethacrylate (EDMA) as the cross linking monomer, with two small drug molecules, theophylline and diazepam, as template molecules.[5] These structures were able to differentiate between close analogues of the template, exhibiting properties similar to natural antibodies and thus representing a remarkable demonstration of the potential of molecular imprinting. Since then, a plethora of new systems has been developed on the basis of different functional monomers, cross-linkers, and porogens in various formulations and with applications ranging from chromatographic stationary bases to immunoassays and drug delivery.[1]

Although significant progress has been made in the development of these novel materials, more rational strategies for their design would require a better understanding of imprinted structure formation, binding, and recognition phenomena on the molecular level.[6] Fundamental questions exist concerning the topology of the imprinted space; the structure, location, and functionality of binding sites; and the influence of template molecular/supramolecular structure on molecular recognition. Some of these issues have been recently considered using computer simulations. For example, recently Chianella and coworkers employed energy minimization methods to quantify interactions between various monomers and imprint molecules.[7,8] These calculations were used as a screening tool to select monomers for polymer synthesis and, in particular, to identify the best monomers for complexation with creatine, ephedrine, and microcystin-LR.[7] Pavel and Lagowski applied the molecular dynamics method to calculate interaction energies in different monomer−imprint mixtures and also extended this approach to small polymerized clusters as model porous materials.[9] Monti et al. developed a computational approach based on the combination of molecular dynamics, molecular mechanics, and binding protocols to investigate the formation of possible imprinted structures in the presence of theophylline.[10] Although some interesting insights have been gained, most of these efforts suffer from two major drawbacks. The first drawback is the focus on binding within a single cavity. Issues related to the heterogeneity of binding sites, binding phenomena over a range of concentration regimes, and accessibility of pore space thus remain beyond the scope of these models. Simulation of a realistic imprinted structure would require employing a mixture of the polymer precursor, template, solvent, and porogen species (depending on the level of realism); the resulting structure would serve as a model porous material and would be used in a series of adsorption simulations (for example, via

† Part of the "Keith E. Gubbins Festschrift".

* To whom correspondence should be addressed. E-mail: Lev.Sarkisov@ed.ac.uk.

‡ University of Edinburgh.

§ Yale University.

10.1021/jp073536g CCC: $37.00
Published on Web 10/25/2007

grand canonical Monte Carlo). Owing to finite size effects, the calculated adsorption isotherm is specific for a particular matrix realization. Therefore, adsorption isotherms must be calculated for several matrix realizations to obtain average properties. Finally, in all these steps, the scale of the system must be representative of a disordered porous structure and therefore significantly larger than that in the aforementioned studies. This latter feature presents a daunting computational task for atomistically detailed models and potentials. The second drawback is the neglect of entropic effects. In particular, the free energy of binding remains elusive in previous computer simulations, and the binding selectivity analysis is usually reduced to a simplified scoring function approach based on the internal energy of complexation. Calculation of free energy is a recognized challenge in computer simulations; current methods such as perturbation theories or thermodynamic integration require construction of pathways between states with known properties. Clearly, if a large range of systems is to be considered, these approaches can become computationally demanding.

A different approach is offered by modern integral equation theories of fluids confined within a disordered porous media. At the heart of these theoretical approaches is the notion that a disordered porous structure can be modeled as a system of quenched particles.[11−37] A theoretical description of a fluid confined in such a matrix was first proposed by Madden and Glandt, who suggested that the classical Ornstein−Zernike equation for bulk fluids and mixtures can be extended to describe quenched−annealed systems.[11,12] This approach was further refined by Given and Stell[14,16,18] and Rosinberg et al.,[19] who developed a more general formalism based on the replica method. The replica Ornstein−Zernike (ROZ) equations of Given and Stell are universally accepted as correct and provide the most general, fundamental description of structural properties of confined fluids. These theories are however approximate. Thermodynamic inconsistencies arise from the approximate nature of the classical closures such as Percus−Yevick (PY), hypernetted chain (HNC), etc., as is well-known from theories of bulk fluids and mixtures. These inconsistencies seem to be further magnified within the ROZ theory of confined fluids. As a result, for a given system, different closures predict different structural properties with various degrees of accuracy when compared to simulation (see, e.g., Lomba et al.[16] and Meroni et al.[24]). Furthermore, thermodynamic properties from integral equation methods depend on the particular route of calculation. For example, virial and compressibility routes lead to different values of pressure. Several recent studies have been dedicated to understanding the relative accuracy of the various closures in the ROZ description of confined fluids and to finding more efficient, consistent routes to the thermodynamic properties of confined fluids via the correlation functions.[29,37]

One particularly important outcome of these studies is a direct method for the excess chemical potential of a confined fluid. In general, there has been a sustained interest in developing closed, analytical formulas for the chemical potential. Such an approach would alleviate the need for computationally cumbersome integration protocols as needed, for example, in the compressibility route. A number of proposed theoretical approaches are rooted in the Kirkwood particle coupling method.[38,39] The idea is to relate the excess chemical potential of a fluid to a process of gradual turning on (or coupling) the interactions between a test particle and the system. Direct application of the Kirkwood method requires several calculations at different degrees of coupling between the test particle and the system. However, for approximate closure relations, it is possible to obtain closed, explicit formulas requiring only the system conditions (such as temperature and density). This approach was developed by Morita for the HNC closure,[40,41] and by Lee for the PY and HNC2 (a modified HNC) closures.[42] A series of generalizations then followed, including contributions from Morita and Hiroike,[41] Verlet and Levesque,[43] and Kjellander and Sarman.[44] Most of the generalizations, however, still contained terms that required gradual turning on and thus integration. Finally, Lee revisited the issue and developed a general explicit and closed formula for the excess chemical potential, which subsequently has been applied to investigate pure fluids and mixtures, both simple and molecular.[45] Later, Fernaud and co-workers employed this method to calculate the chemical potential of an inclusion gas in a random porous system.[29] Another example is provided by Kovalenko and Hirata, who developed a replica reference interaction site model for a molecular fluid confined in a disordered microporous material.[46] In their work, the excess chemical potential of the confined species was calculated using the partially linearized HNC (PLHNC)[47,48] closure with a set of expressions similar to that of Singer and Chandler.[49] Mixtures of simple fluids in random pores have been also recently considered.[34]

An explicit, closed formula for the excess chemical potential would be particularly valuable in studies of templated materials as it would provide direct access to their most fundamental characteristic, the free energy of binding. We are thereby motivated to explore in greater detail a general theoretical model of templated materials that we proposed in a previous publication.[50] The idea of the model is to reflect the actual process of templated material formation. The first step involves an equilibrated mixture of template and matrix species. The mixture is then quenched, and the template molecules are removed. The resulting structure of the quenched matrix component serves as the model porous material. Van Tassel and co-workers have developed an extended set of ROZ equations to describe correlations in this matrix−template−adsorbate system.[35,36,51] For simple species, interacting with hard-sphere and Lennard-Jones-like potentials, they observed that the presence of a template enhances adsorption and that the magnitude of the effect strongly depends on the template/matrix composition ratio and on the size of the template. However, as expected, no molecular recognition effect could be captured in a system of simple particles. Recently, a different theoretical model has been proposed, where the effect of templating is captured through a special cavity potential.[52] In our previous publication, we extended the model of Van Tassel and co-workers model to molecular species. The developed theory combines the original ROZ method with the reference interaction site model (RISM) in a fashion similar to that suggested by Kovalenko and Hiarata[46] and applies the resulting formalism to a ternary matrix−template−adsorbate system. The focus of the previous work was on geometrical effects, where we explored a range of systems with purely repulsive interactions. In particular, we investigated adsorption of rigid linear chains, clusters, and molecules of other shapes in matrices templated with these species. The most general conclusion of the previous work is that it is not possible for a purely geometrical model to yield a molecular recognition effect; instead, a number of nontrivial entropic factors dictate system behavior.

In this work, we consider molecular species interacting with a Lennard-Jones-like potential, accounting for both attraction and repulsion between molecular pairs. We extend the method of Fernaud and co-workers[29] for the excess chemical potential

to molecular fluids confined in imprinted structures and examine its scope and applicability in combination with a group of closures requiring no additional parameter adjustments. We compare the results to those generated by Monte Carlo simulation and to those predicted from the compressibility route.

2. General Theory

The idea of the ROZ method is to relate the thermodynamic properties of a nonequilibrium quenched−annealed system to an equilibrium system of matrix, template, and *s* identical copies of the adsorbate, each of which interacts with the matrix components but not with other replicas or the template. All thermodynamic properties of a quenched−annealed system can then be derived from those of the replica system by considering it in the limit of $s \rightarrow 0$. The relation between the replica and the quenched−annealed system is particularly simple for pair correlation functions which can be written in the most general way:

$$\rho_{ij}(\vec{\mathbf{r}}_1,\vec{\mathbf{r}}_2) = \rho_{ij}^{\mathrm{rep}}(\vec{\mathbf{r}}_1,\vec{\mathbf{r}}_2;s=0) \quad (1)$$

where $\rho_{ij}(\vec{\mathbf{r}}_1,\vec{\mathbf{r}}_2)$ and $\rho_{ij}^{\mathrm{rep}}(\vec{\mathbf{r}}_1,\vec{\mathbf{r}}_2;\ s=0)$ are pair distribution functions between a particle of species *i* located at position $\vec{\mathbf{r}}_1$ and a particle of species *j* located at position $\vec{\mathbf{r}}_2$ in the quenched−annealed system and the replica system, respectively. This relation is also valid for total, direct, and other correlation functions. In our previous study, we employed a RISM approach to formulate site−site Ornstein−Zernike equations relating total and direct correlation functions for a quenched−annealed system of molecular matrix, template, and fluid components:[50]

$$h_{00}^{\lambda\eta} = \omega_0^{\lambda\nu} \otimes c_{00}^{\nu\tau} \otimes \omega_0^{\tau\eta} + \rho_0\omega_0^{\lambda\nu} \otimes c_{00}^{\nu\tau} \otimes h_{00}^{\tau\eta} + \rho_{0'}\omega_0^{\lambda\nu} \otimes c_{00'}^{\nu\tau} \otimes h_{0'0}^{\tau\eta} \quad (2)$$

$$h_{00'}^{\lambda\eta} = \omega_0^{\lambda\nu} \otimes c_{00'}^{\nu\tau} \otimes \omega_{0'}^{\tau\eta} + \rho_0\omega_0^{\lambda\nu} \otimes c_{00}^{\nu\tau} \otimes h_{00'}^{\tau\eta} + \rho_{0'}\omega_0^{\lambda\nu} \otimes c_{00'}^{\nu\tau} \otimes h_{0'0'}^{\tau\eta} \quad (3)$$

$$h_{0'0'}^{\lambda\eta} = \omega_{0'}^{\lambda\nu} \otimes c_{0'0'}^{\nu t} \otimes \omega_{0'}^{\tau\eta} + \rho_0\omega_{0'}^{\lambda\nu} \otimes c_{0'0}^{\nu\tau} \otimes h_{00'}^{\tau\eta} + \rho_{0'}\omega_{0'}^{\lambda\nu} \otimes c_{0'0'}^{\nu\tau} \otimes h_{0'0'}^{\tau\eta} \quad (4)$$

$$h_{01}^{\lambda\eta} = \omega_0^{\lambda\nu} \otimes c_{01}^{\nu\tau} \otimes \omega_1^{\tau\eta} + \rho_0\omega_0^{\lambda\nu} \otimes c_{00}^{\nu\tau} \otimes h_{01}^{\tau\eta} + \rho_{0'}\omega_0^{\lambda\nu} \otimes c_{00'}^{\nu\tau} \otimes h_{0'1}^{\tau\eta} + \rho_1\omega_0^{\lambda\nu} \otimes c_{01}^{\nu\tau} \otimes h_c^{\tau\eta} \quad (5)$$

$$h_{0'1}^{\lambda\eta} = \omega_{0'}^{\lambda\nu} \otimes c_{0'1}^{\nu\tau} \otimes \omega_1^{\tau\eta} + \rho_0\omega_{0'}^{\lambda\nu} \otimes c_{0'0}^{\nu\tau} \otimes h_{01}^{\tau\eta} + \rho_{0'}\omega_{0'}^{\lambda\nu} \otimes c_{0'0'}^{\nu\tau} \otimes h_{0'1}^{\tau\eta} + \rho_1\omega_{0'}^{\lambda\nu} \otimes c_{0'1}^{\nu\tau} \otimes h_c^{\tau\eta} \quad (6)$$

$$h_{11}^{\lambda\eta} = \omega_1^{\lambda\nu} \otimes c_{11}^{\nu\tau} \otimes \omega_1^{\tau\eta} + \rho_0\omega_1^{\lambda\nu} \otimes c_{10}^{\nu\tau} \otimes h_{01}^{\tau\eta} + \rho_{0'}\omega_1^{\lambda\nu} \otimes c_{10'}^{\nu\tau} \otimes h_{0'1}^{\tau\eta} + \rho_1\omega_1^{\lambda\nu} \otimes c_c^{\nu\tau} \otimes h_{11}^{\tau\eta} + \rho_1\omega_1^{\lambda\nu} \otimes c_{\mathrm{B}}^{\nu\tau} \otimes h_c^{\tau\eta} \quad (7)$$

$$h_c^{\lambda\eta} = \omega_1^{\lambda\nu} \otimes c_c^{\nu\tau} \otimes \omega_1^{\tau\eta} + \rho_1\omega_1^{\lambda\nu} \otimes c_c^{\nu\tau} \otimes h_c^{\tau\eta} \quad (8)$$

where $h_{ij}^{\lambda\eta}(c_{ij}^{\lambda\eta})$ are total (direct) site−site correlation functions for species *i* and *j*, $h_{\mathrm{B}}^{\lambda\eta}(r)$ and $c_{\mathrm{B}}^{\lambda\eta}(r)$ are the site−site blocking correlation functions, and $h_C^{\lambda\eta}(r) = h_{11}^{\lambda\eta}(r) - h_{\mathrm{B}}^{\lambda\eta}(r)$ and $c_{\mathrm{C}}^{\lambda\eta}(r) = c_{11}^{\lambda\eta}(r) - c_{\mathrm{B}}^{\lambda\eta}(r)$ are the site−site connected correlation functions as discussed elsewhere.[14,18,19] 0, 0′, and 1 subscripts label matrix, template, and adsorbed fluid components, respectively. $\omega_i^{\lambda\eta}$ is the intramolecular correlation function for sites λ and η of a molecule of species *i*. Finally, for the sake of simplicity, we assign the symbol ⊗ to represent a convolution of the correlation functions in real space *and* a summation over proper site indices. This system of equations (eqs 2−8) can be solved in combination with a particular closure relation. Here we adopt a numerical procedure developed by Labik and co-workers based on the Newton−Raphson method.[53]

To complete the theoretical description of adsorption in imprinted materials, we next link these correlation functions to the chemical potential of the confined fluid. In our previous study, we have developed an approach based on the compressibility route.[50] Here, we only briefly review the basic steps of the approach and refer the reader to the original publication for the details.

The total chemical potential of confined species is given by

$$\beta\mu_1(\rho_0,\rho_{0'},\rho_1) = \beta\mu_1^{\mathrm{ex}}(\rho_0,\rho_{0'},\rho_1) + \ln(\rho_1\Lambda_1{}^3/q_1^{\mathrm{rot}}) \quad (9)$$

where $\mu_1^{\mathrm{ex}}(\rho_0,\rho_{0'},\rho_1)$ is the excess chemical potential at ρ_0, $\rho_{0'}$, and the ρ_1 densities of the matrix, template, and adsorbate, correspondingly, $\Lambda_1$is the de Broglie wavelength (taken to be equal to σ), and q_1^{rot} is the ideal gas rotational partition function (taken to be unity). The excess chemical potential can be written as

$$\beta\mu_1^{\mathrm{ex}}(\rho_0,\rho_{0'},\rho_1) = \beta\mu_1^{\mathrm{ex}}(\rho_0,\rho_{0'},\rho_1=0) + \int_0^{\rho_1}\left(\frac{\partial\beta\mu_1^{\mathrm{ex}}}{\partial\rho_1}\right)_{\rho_0,\rho_{0'}} \mathrm{d}\rho_1' \quad (10)$$

where the first term on the right corresponds to the excess of chemical potential as a result of matrix and template species present at $\rho_1 = 0$ and the second term considers the contribution of the adsorbed fluid to the excess chemical potential compared to that at $\rho_1 = 0$. The second term can be calculated as

$$\int_0^{\rho_1}\left(\frac{\partial\beta\mu_1^{\mathrm{ex}}}{\partial\rho_1}\right)_{\rho_0,\rho_{0'}} \mathrm{d}\rho_1' = -\int_0^{\rho_1} \hat{c}_c^{\lambda\eta}(\rho_0,\rho_{0'},\rho_1')\,\mathrm{d}\rho_1' \quad (11)$$

whereas for the first term we have

$$\beta\mu_1^{\mathrm{ex}}(\rho_0,\rho_{0'},\rho_1=0) = \int_0^{\rho_{0'}}\left.\frac{\partial\beta\mu_1^{\mathrm{ex}}}{\partial\rho_{0'}}\right|_{\rho_0=0,\rho_{0'},\rho_1=0} \mathrm{d}\rho_{0'}' + \int_0^{\rho_0}\left.\frac{\partial\beta\mu_1^{\mathrm{ex}}}{\partial\rho_0}\right|_{\rho_{0'},\rho_{0'},\rho_1=0} \mathrm{d}\rho_0' \quad (12)$$

The first term on the right side of eq 12 is trivially zero, as integration takes place at zero matrix density $\rho_0 = 0$. An appropriate expression for the second term on the right side of eq 12 was derived previously.[50] This expression included only total site−site correlation functions and species densities. This approach was combined with the Percus−Yevick closure (for brevity we label this method "PY-comp" in the discussion and figures that follow) and applied to hard-sphere-site systems confined in the templated hard-sphere matrix. Although a reasonable qualitative behavior was obtained, two weaknesses of the approach were apparent. First, the method requires two numerical integrations of the terms contributing to the excess chemical potential. Second, eq 12 can be recast to change the order of integration with respect to matrix and template densities, and it was observed that the numerical results for the chemical potential of adsorbate at infinite dilution depended on the integration protocol.[50] This is just another manifestation of the thermodynamic inconsistencies arising from the approximate nature of the available closures.

An alternative approach has been recently developed over a series of publications, which offers a procedure for the direct evaluation of the excess chemical potential at a given species density.[29,45] Consider an equilibrium mixture of matrix, template, and s replicas of adsorbate. The excess chemical potential of adsorbate species can be expressed via the generalized Kirkwood equation:

$$\beta\mu_1^{\mathrm{ex,rep}}(s) = \rho_0[10]_s + \rho_{0'}[10']_s + \rho_1[11]_s + (s-1)\rho_1[12]_s \quad (13)$$

where superscript rep signifies properties of the replica system and each term $[ij]_s$ is a contribution to the excess chemical potential of species i resulting from the presence of species j in a system of $(s+2)$ components. Each of these contributions can be calculated using the Kirkwood coupling procedure,[38,39]

$$[ij]_s = \sum_{\lambda=1}^{M_i}\sum_{\eta=1}^{M_j}\int_0^1 \mathrm{d}\xi_{ij}\, 4\pi \int_0^\infty \mathrm{d}r\, r^2 \frac{\partial\beta u_{ij}^{\lambda\eta}(r,\xi_{ij})}{\partial\xi_{ij}} g_{ij}^{\lambda\eta,\mathrm{rep}}(r,\xi_{ij},s) \quad (14)$$

where M_i is the number of interaction sites in a molecule of species i, $u_{ij}^{\lambda\eta}(r,\xi_{ij})$ is the pair interaction energy between site λ on a molecule of type i and site η on a molecule of type j, $g_{ij}^{\lambda\eta,\mathrm{rep}}(r,\xi_{ij},s)$ is a pair distribution function between a site on the scaled molecule of species i and a site on a full molecule of species j in the replica system of s replicas, and $u_{ij}^{\lambda\eta}(r,\xi_{ij})$ is also a continuous function of the coupling parameter ξ_{ij},

$$u_{ij}^{\lambda\eta}(r,\xi_{ij}) = \begin{cases} u_{ij}^{\lambda\eta}(r) & \xi_{ij}=1 \\ 0 & \xi_{ij}=0 \end{cases} \quad (15)$$

so that when $\xi_{ij}=0$, the test particle of species i is absent, and when $\xi_{ij}=1$, it is fully present. An equilibrium replica mixture exhibits no interactions between two distinct replicas, i.e., $u_{12}=0$. Thus, for different replica species, $\partial\beta u_{12}^{\lambda\eta}(r,\xi_{12})/\partial\xi_{12}=0$ irrespective of the particular functional dependence of $u_{12}^{\lambda\eta}(r,\xi_{12})$ on ξ_{12} and the last term in eq 13 vanishes. By the same token, the second contribution coming from the presence of template molecules also vanishes, since $u_{10'}=0$. We note that even though no interaction exists between different replica species or between a replica and the template component, the correlation functions $h_{12}^{\lambda\eta,\mathrm{rep}}$ and $h_{10'}^{\lambda\eta,\mathrm{rep}}$ are in general nonzero. Although there is no explicit contribution coming from replicas or template species in eq 13, their contributions are present in the $[10]_s$ and $[11]_s$ terms, as the correlation functions in those expressions are affected by the presence of other replicas and template species. Thus, eq 13 simplifies to

$$\beta\mu_1^{\mathrm{ex,rep}}(s) = \rho_0[10]_s + \rho_1[11]_s \quad (16)$$

Each individual term in this equation can be evaluated using an explicit, closed formula for the excess chemical potential of a component in a mixture of molecular fluids developed by Lee,[45]

$$[ij]_s = \sum_{\lambda=1}^{M_i}\sum_{\eta=1}^{M_j} 4\pi \int_0^\infty \mathrm{d}r\, r^2 \frac{(h_{ij}^{\lambda\eta,\mathrm{rep}})^2}{2} - \frac{h_{ij}^{\lambda\eta,\mathrm{rep}}c_{ij}^{\lambda\eta,\mathrm{rep}}}{2} - c_{ij}^{\lambda\eta,\mathrm{rep}} + B_{ij}^{\lambda\eta,\mathrm{rep}} + h_{ij}^{\lambda\eta,\mathrm{rep}}B_{ij}^{\lambda\eta,\mathrm{rep}} - \frac{h_{ij}^{\lambda\eta,\mathrm{rep}}}{\gamma_{ij}^{\lambda\eta,\mathrm{rep}}}\int_0^{\gamma_{ij}^{\lambda\eta}} \mathrm{d}\gamma_{ij}^{\lambda\eta,\mathrm{rep}}\, B_{ij}^{\lambda\eta,\mathrm{rep}}(\gamma_{ij}^{\lambda\eta,\mathrm{rep}}) \quad (17)$$

where $h_{ij}^{\lambda\eta,\mathrm{rep}}$ is the total site−site correlation function, $c_{ij}^{\lambda\eta,\mathrm{rep}}$ is the direct site−site correlation function, $\gamma_{ij}^{\lambda\eta,\mathrm{rep}} = h_{ij}^{\lambda\eta,\mathrm{rep}} - c_{ij}^{\lambda\eta,\mathrm{rep}}$, and $B_{ij}^{\lambda\eta,\mathrm{rep}}$ is the bridge function in the replica system. In this and the following equations, it is understood that all the involved pair correlation functions are functions of the distance between the particles or sites $X \equiv X(r)$, where X can be h, c, γ, or B.

The transition from an equilibrium replica system to a quenched−annealed system is accomplished by setting the limit $s=0$. The final expression for the excess chemical potential of a fluid confined in a templated porous structure is

$$\beta\mu_1^{\mathrm{ex}} = \rho_0[10] + \rho_1[11]$$

$$[ij] = \sum_{\lambda=1}^{M_i}\sum_{\eta=1}^{M_j} 4\pi \int_0^\infty \mathrm{d}r\, r^2 \frac{(h_{ij}^{\lambda\eta})^2}{2} - \frac{h_{ij}^{\lambda\eta}c_{ij}^{\lambda\eta}}{2} - c_{ij}^{\lambda\eta} + B_{ij}^{\lambda\eta} + h_{ij}^{\lambda\eta}B_{ij}^{\lambda\eta} - \frac{h_{ij}^{\lambda\eta}}{\gamma_{ij}^{\lambda\eta}}\int_0^{\gamma_{ij}^{\lambda\eta}} \mathrm{d}\gamma_{ij}^{\lambda\eta}\, B_{ij}^{\lambda\eta}(\gamma_{ij}^{\lambda\eta}) \quad (18)$$

and total and direct correlation functions are solutions of eqs 2−8. The remaining unknowns in the eq 18 are the terms involving the bridge function which will depend on a particular closure.

3. Closure Relations

Percus−Yevick Approximation (PY).[54] In our previous publication, we employed the well-established PY closure, which is known to perform reasonably well while retaining mathematical simplicity:

$$g_{ij}^{\lambda\eta} = [f_{ij}^{\lambda\eta}+1][\gamma_{ij}^{\lambda\eta}+1] \quad (19)$$

where $f_{ij}^{\lambda\eta} = \exp(-\beta u_{ij}^{\lambda\eta}) - 1$ is the Mayer function. Note that using the Percus−Yevick PY closure leads to $c_{\mathrm{B}} \equiv 0$ or alternatively $c_{11} = c_{\mathrm{C}}$, as has been previously discussed. Also, from the form of the potential (specifically, from the absence of any interaction between template and adsorbate components) and from the PY closure, it follows that $c_{0'1} \equiv 0$. In the PY approximation, the expression for the bridge function is

$$B_{ij}^{\lambda\eta} = \ln(1+\gamma_{ij}^{\lambda\eta}) - \gamma_{ij}^{\lambda\eta} \quad (20)$$

The last term in the brackets in eq 18 is then

$$\int_0^{\gamma_{ij}^{\lambda\eta}} \mathrm{d}\gamma_{ij}^{\lambda\eta}\, B_{ij}^{\lambda\eta}(\gamma_{ij}^{\lambda\eta}) = \int_0^{\gamma_{ij}^{\lambda\eta}} \mathrm{d}\gamma_{ij}^{\lambda\eta}\, \{\ln(1+\gamma_{ij}^{\lambda\eta}) - \gamma_{ij}^{\lambda\eta}\} = \left[-\frac{(\gamma_{ij}^{\lambda\eta})^2}{2} + (1+\gamma_{ij}^{\lambda\eta})\ln(1+\gamma_{ij}^{\lambda\eta}) - \gamma_{ij}^{\lambda\eta}\right] \quad (21)$$

This along with eq 20 substituted in eq 18 results in

$$[ij] = \sum_{\lambda=1}^{M_i}\sum_{\eta=1}^{M_j} 4\pi \int_0^\infty \mathrm{d}r\, r^2 \left[\ln(1+\gamma_{ij}^{\lambda\eta})\cdot\left(\frac{\gamma_{ij}^{\lambda\eta} - h_{ij}^{\lambda\eta}}{\gamma_{ij}^{\lambda\eta}}\right)\right] \quad (22)$$

This expression for simple bulk liquids was first obtained by Lee and consequently applied to bulk fluids and mixtures.[45]

Soft Mean Spherical Approximation (SMSA). Soft mean spherical approximation can be viewed as a generalized mean spherical approximation (MSA) extended to the systems with soft core and attractive potentials.[55] The idea is to separate the intermolecular potential into a purely repulsive and a purely attractive part

$$u_{ij}^{\lambda\eta} = \chi_{ij}^{\lambda\eta} + \upsilon_{ij}^{\lambda\eta} \quad (23)$$

$$\chi_{ij}^{\lambda\eta}(r) = \begin{cases} u_{ij}^{\lambda\eta}(r) - u_{ij}^{\lambda\eta}(r_{\min}) & r \le r_{\min} \\ 0 & r > r_{\min} \end{cases} \quad (24)$$

$$\upsilon_{ij}^{\lambda\eta}(r) = \begin{cases} u_{ij}^{\lambda\eta}(r_{min}) & r \le r_{\min} \\ u_{ij}^{\lambda\eta}(r) & r > r_{\min} \end{cases} \quad (25)$$

where $\chi_{ij}^{\lambda\eta}$ is the repulsive part, $\upsilon_{ij}^{\lambda\eta}$ is the attractive part, and $r_{\min}$ is the location of the potential minimum. In this case, we can define a new function $\Gamma_{ij}^{\lambda\eta}(r)$, such that

$$\Gamma_{ij}^{\lambda\eta} = -\beta\upsilon_{ij}^{\lambda\eta} + \gamma_{ij}^{\lambda\eta} \quad (26)$$

and the resulting closure resembles the PY approximation

$$g_{ij}^{\lambda\eta} = [\exp(-\beta\chi_{ij}^{\lambda\eta})][\Gamma_{ij}^{\lambda\eta} + 1] \quad (27)$$

Indeed, this function will reduce to the PY closure at negligible attractive tail potentials $\upsilon_{ij}^{\lambda\eta}$. For potentials where the repulsive part $\chi_{ij}^{\lambda\eta}$ is a hard-sphere repulsion ($\chi_{ij}^{\lambda\eta} = \infty$ for $r < \sigma$), the SMSA closure is reduced to the classical MSA.[56]

The bridge function for the SMSA closure is

$$B_{ij}^{\lambda\eta} = \ln(1+\Gamma_{ij}^{\lambda\eta}) - \Gamma_{ij}^{\lambda\eta} \quad (28)$$

Then,

$$\int_0^{\gamma_{ij}^{\lambda\eta}} \mathrm{d}\gamma_{ij}^{\lambda\eta}\, B_{ij}^{\lambda\eta}(\gamma_{ij}^{\lambda\eta}) = \int_0^{\gamma_{ij}^{\lambda\eta}} \mathrm{d}\gamma_{ij}^{\lambda\eta}\, \{\ln(1+\Gamma_{ij}^{\lambda\eta}) - \Gamma_{ij}^{\lambda\eta}\} = -\frac{(\gamma_{ij}^{\lambda\eta})^2}{2} + (1+\Gamma_{ij}^{\lambda\eta})\ln(1+\Gamma_{ij}^{\lambda\eta}) - (1-\beta\upsilon_{ij}^{\lambda\eta})\ln(1-\beta\upsilon_{ij}^{\lambda\eta}) - \gamma_{ij}^{\lambda\eta} + \beta\upsilon_{ij}^{\lambda\eta}\gamma_{ij}^{\lambda\eta} \quad (29)$$

Note that, also like the PY closure, this approximation also leads to $c_B \equiv 0$ (or $c_{11} = c_C$) and $c_{0'1} \equiv 0$.

Hypernetted Chain Approximation (HNC).[40,41] Hypernetted chain approximation can be formulated as

$$g_{ij}^{\lambda\eta} = \exp[-\beta u_{ij}^{\lambda\eta} + \gamma_{ij}^{\lambda\eta}] \quad (30)$$

$$B_{ij}^{\lambda\eta} = 0 \quad (31)$$

This approximation results in vanishing of the last term in brackets in eq 18, and therefore the individual terms in eq 18 become

$$[ij] = \sum_{\lambda=1}^{M_i}\sum_{\eta=1}^{M_j} 4\pi \int_0^\infty \mathrm{d}r\, r^2 \left[\frac{(h_{ij}^{\lambda\eta})^2}{2} - \frac{h_{ij}^{\lambda\eta}c_{ij}^{\lambda\eta}}{2} - c_{ij}^{\lambda\eta}\right] \quad (32)$$

The expression within the brackets in eq 32 was originally obtained in a general form by Morita.[40] In the context of molecular liquids, a similar expression for a polyatomic solute in a solvent was obtained by Singer and Chandler for bulk molecular fluids.[49]

Partially Linearized Hypernetted Chain Approximation (PLHNC).[47,48] It has been noted that the standard closures exhibit a range of limitations when applied to ROZ formalism. HNC proves to be extremely difficult to converge under conditions of interest, whereas PY and MSA closures tend to produce unphysical negative values of the pair correlation function. In an attempt to combine the advantages of HNC and MSA closures, Kovalenko and Hirata developed an alternative closure called partially linearized hypernetted chain approximation (PLHNC).[47,48] In this closure, we define a function similar to the function in the MSA closure,

$$G_{ij}^{\lambda\eta} = -\beta u_{ij}^{\lambda\eta} + \gamma_{ij}^{\lambda\eta} \quad (33)$$

and the PLHNC approximation then reads

$$g_{ij}^{\lambda\eta} = \begin{cases} \exp(G_{ij}^{\lambda\eta}) & G_{ij}^{\lambda\eta} \le 0 \\ 1 + G_{ij}^{\lambda\eta} & G_{ij}^{\lambda\eta} > 0 \end{cases} \quad (34)$$

It is easy to see that the first part of the closure is the HNC relation applied to $h_{ij}^{\lambda\eta} < 0$ (depletion regions) whereas the second part is MSA applied to $h_{ij}^{\lambda\eta} > 0$ (enrichment) regions. The pair correlation function and its first derivative are continuous at the joint point $G = 0$ by construction. The following expression has been derived for individual terms in eq 18:

$$[ij] = \sum_{\lambda=1}^{M_i}\sum_{\eta=1}^{M_j} 4\pi \int_0^\infty \mathrm{d}r\, r^2 \left[\frac{(h_{ij}^{\lambda\eta})^2\Theta(-h_{ij}^{\lambda\eta})}{2} - \frac{h_{ij}^{\lambda\eta}c_{ij}^{\lambda\eta}}{2} - c_{ij}^{\lambda\eta}\right] \quad (35)$$

This equation is different from the equation for the HNC closure only by the Heaviside step function $\Theta(-h_{ij}^{\lambda\eta})$, which is switched off in the regions where $h_{ij}^{\lambda\eta} > 0$ and the MSA closure is applied.

It is important to note that, in their original work, Kovalenko and Hirata also included a contribution to the excess chemical potential coming from the blocking correlation functions.[46] For the blocking functions, the pure HNC closure was used along with an expression for the excess chemical potential identical to eq 32. We, however, chose not include this contribution (or an analogous contribution coming from the template−adsorbate correlations) for the reasons explained with eq 14.

Martynov−Sarkisov Approximation (MS).[57] In the context of confined fluids, the Martynov−Sarkisov closure has been recently applied by Pillicane and co-workers to the symmetrical binary mixture of nonadditive hard spheres in a disordered hard-sphere matrix.[34] In the MS approximation, the pair site−site distribution function is given by

$$g_{ij}^{\lambda\eta} = \exp(-\beta u_{ij}^{\lambda\eta} + (1+2\gamma_{ij}^{\lambda\eta})^{1/2} - 1) \quad (36)$$

with the bridge function formulated as

$$B_{ij}^{\lambda\eta} = (1+2\gamma_{ij}^{\lambda\eta})^{1/2} - \gamma_{ij}^{\lambda\eta} - 1 \quad (37)$$

and

$$\int_0^{\gamma_{ij}^{\lambda\eta}} \mathrm{d}\gamma_{ij}^{\lambda\eta}\, B(\gamma_{ij}^{\lambda\eta}) = \frac{1}{3}(1+2\gamma_{ij}^{\lambda\eta})^{3/2} - \frac{1}{3} - \frac{(\gamma_{ij}^{\lambda\eta})^2}{2} - \gamma_{ij}^{\lambda\eta} \quad (38)$$

4. Systems

Three systems are considered. In the first system (system 1), each of the species, i.e., the matrix, template, and adsorbate, is a simple fluid of spherical particles (Figure 1, left). These particles are of the same type for all the species, they have a diameter σ, and interact with a truncated Lennard-Jones perturbation potential, considered in our earlier studies.

$$u(r)/k_BT = \begin{cases} \infty & r < \sigma \\ -\epsilon/k_BT & \sigma \le r < 2^{1/6}\sigma \\ \dfrac{4\epsilon}{k_BT}\left[\left(\dfrac{\sigma}{r}\right)^{12} - \left(\dfrac{\sigma}{r}\right)^{6}\right] & 2^{1/6}\sigma \le r < 2.5\sigma \\ 0 & r \ge 2.5\sigma \end{cases} \quad (39)$$

Here ϵ/k_BT is the well depth of the potential, taken here to be equal 0.5 for all species.

In the second system (system 2), the matrix component is a simple fluid of spherical particles as before. Template and adsorbate species are clusters of particles, each of the same type as for the matrix species. In principle, the theory is not limited in terms of geometry and size of the molecular species it can describe. Here, we focus only on one case, where both the template and the adsorbate are rigid, linear chains of tangent spheres. All interactions are truncated Lennard-Jones perturbation interactions, as given in eq 39, with a well depth ϵ/k_BT of 0.5. This system is schematically depicted in the center of Figure 1.

Finally, in system 3, the structure of the species is the same as in system 2, but the interaction arrangement is different. In system 3, all sites interact via a hard-sphere potential and some of the matrix sites additionally interact with one of the sites in the linear chain molecule via an attractive L-J-like potential (eq 39) with a well depth ϵ/k_BT of 2.0. This deeper potential (compared to that in system 1 and system 2) imitates the interaction between functional monomers in the precursor mixture and functional groups of the template molecule. Since the only attractive interactions here are between template/adsorbate and matrix, we are not at this stage considering competitive associations. The location of the functional group (or more precisely the functional site) in the linear chain molecule is either at the center (we call these molecules ABA) or at the terminus of the chain (AAB molecules). One-third of the matrix particles (these are the functional monomers) exhibits this attractive interaction, thus making the interaction stoichiometric. On the right of Figure 1, we schematically depict the formation of a matrix templated with AAB species.

In templated systems, we consider the matrix density as $\rho_0\sigma^3 = (N_0/V)\sigma^3 = 0.5$ and the template density is $M_{0'}\rho_{0'}\sigma^3 = (M_{0'}N_{0'}/V)\sigma^3 = 0.3$, where $M_{0'} = 1$ or 3 is the number of interaction sites in the template molecule. Chemical potentials of adsorbed species are calculated as a function of adsorbed fluid density. This calculation is performed for a range of closures using the approach presented in section 3. In addition, for each system, chemical potentials are calculated using the compressibility route in combination with the PY closure, as described in our previous work. The resulting adsorption isotherms (adsorbed fluid density versus chemical potential) are compared to those calculated via Monte Carlo simulation. Simulation details are presented below.

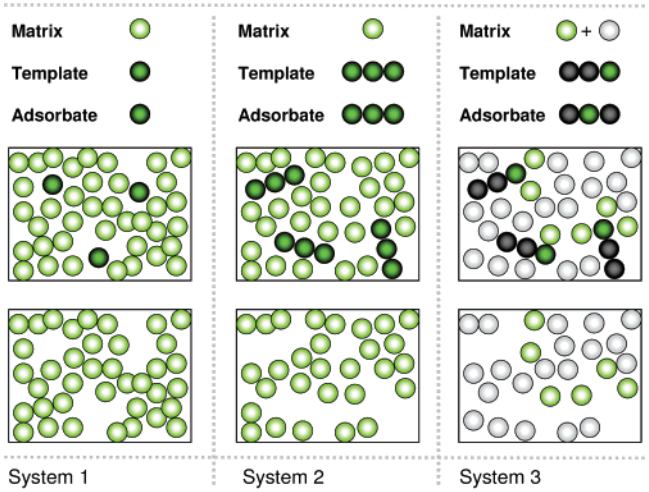

Figure 1. Schematic depiction of the systems considered in this work. System 1 (left) involves simple matrix (light green) and both template and adsorbate (dark green) particles of the same collision diameter σ. System 2 (center) considers a simple fluid matrix (light green) and rigid, three-site linear chains for template and adsorbate. These chains are composed of interaction sites identical to those of the matrix. All interactions in systems 1 and 2 are truncated Lennard-Jones, as given in eq 39. System 3 (right) involves a matrix of simple particles and three-site linear chains as template or adsorbate. The collision diameter of all particles or sites is σ. A truncated Lennard-Jones potential governs interactions between a portion of the matrix particles (functional monomers, shown in green) and a designated site in a chain (functional group, also shown in green). All other interactions are of the hard-sphere type. The position of the functional monomer within a chain may be at the terminal (AAB molecule) or central (ABA molecule) site. The fraction of functional monomers in the matrix fluid is $^1/_3$. The top figures show binary mixtures of monomers and templates for the three systems. The lower figures show the matrix structures following template removal.

5. Simulation

To test the accuracy of our theoretical predictions, we perform computer simulations for the systems described above. We consider a cubic simulation cell with edges of length 10σ and periodic boundary conditions applied in all directions. The binary mixture is equilibrated for ca. 10^8 canonical Monte Carlo moves. Upon equilibration, the template component is removed and the remaining structure serves as the model templated material. For each system, a total of 5 different matrix realizations are generated.

We then perform a grand canonical Monte Carlo simulation of an adsorbed component in each realization. The total number of moves for each run is of the order of 10^8. Translation and rotation attempts are accepted according to the following probability criteria

$$P_{tr} = \min(1, e^{-\beta(U_{new}-U_{old})}) \quad (40)$$

where U_{new} is the new configurational energy of the system after an attempted perturbation and U_{old} is the initial configurational energy. Attempts to insert or delete a molecule are accepted based on the following probability criteria

$$P_{insertion} = \min\left(1, \frac{q_1^{rot} e^{\beta\mu_1} V e^{-\beta(U_{new}-U_{old})}}{(N_1+1)\Lambda_1^{\,3}}\right) \quad (41)$$

$$P_{deletion} = \min\left(1, \frac{N_1\Lambda_1^{\,3} e^{-\beta(U_{new}-U_{old})}}{q_1^{rot} e^{\beta\mu_1} V}\right) \quad (42)$$

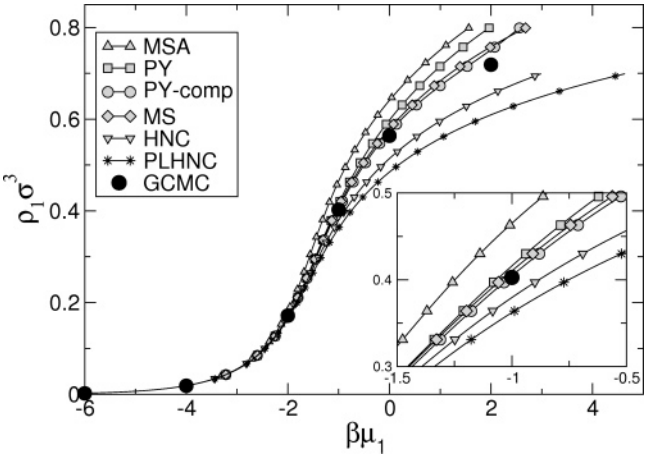

Figure 2. The adsorption isotherms (fluid density $\rho_1\sigma^3 = (N_1/V)\sigma^3$ as a function of the total fluid chemical potential $\beta\mu_1$) for system 1 at zero matrix and template densities (i.e., bulk fluid isotherms). The potential well depth is $\epsilon/k_BT = 0.5$. The figure compares results from the direct method for the excess chemical potential calculation for MSA (triangles), PY (squares), MS (rhombs), HNC (reversed triangles), and PLHNC (stars) closures with the compressibility route results for the PY closure (PY-comp, circles) and grand canonical Monte Carlo simulations (filled circles). The inset shows the expanded region at an intermediate density of the fluid $\rho_1\sigma^3 \sim 0.4$.

where N_1 is the number of fluid molecules in the system, V is the volume of the system, and μ_1 is the chemical potential of the adsorbate. (Note that the de Broglie wavelength, Λ_1, and the ideal gas rotational partition function, q_1^{rot}, are implicitly set to σ and 1, respectively). Attempts to translate, rotate (in the case of molecular species), insert, or delete a particle are weighted equally.

6. Results

We begin our analysis with a special case of system 1, where densities of matrix and template components are equal to zero (i.e., the bulk fluid case). Isotherms calculated using various closures are presented in Figure 2 and compared with the results from simulation. It appears the best agreement is provided by the MS and PY closures in combination with the compressibility route (PY-comp). The order of isotherms from the HNC, MS, and PY closures is in agreement with similar studies on the bulk Lennard-Jones fluid.[58] At a given chemical potential, the density of the fluid predicted from the integral equation theory decreases in the following progression ρ_1 (MSA) > ρ_1 (PY) > ρ_1 (PY-comp) > ρ_1 (MS) > ρ_1 (HNC) > ρ_1 (PLHNC), with the results from GCMC simulations being slightly below those predicted by the MS closure.

In Figure 3, we consider results for a simple fluid confined in a templated matrix (system 1). The order of the adsorption isotherms calculated via the various closure relations remains similar to that for bulk fluid, with the MS closure now generating the best predictions. None of the closures provide satisfactory agreement at higher adsorbed densities. It is important to note that for confined systems, all closures, except for PY and MSA, lead to serious convergence problems at higher densities. As seen from the figure and as expected, this issue is most severe for the HNC closure, and the adsorption isotherm could not be continued beyond the points shown. Although from a convergence perspective PLHNC performs significantly better than HNC, it does not alleviate this issue completely. More encouraging results observed in the original work by Kovalenko and Hirata[46] are likely associated with their advanced solution algorithm involving the modified inversion in the iterative

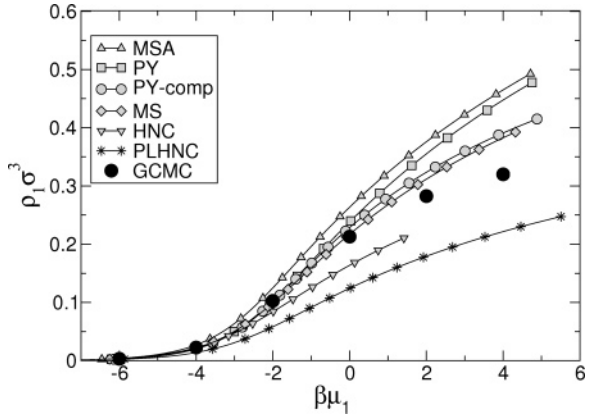

Figure 3. The adsorption isotherms (adsorbate density $\rho_1\sigma^3 = (N_1/V)\sigma^3$ as a function of the total adsorbate chemical potential $\beta\mu_1$) for system 1. The matrix density is $\rho_0\sigma^3 = 0.5$, the template density is $\rho_{0'}\sigma^3 = 0.3$, and the potential well depth is $\epsilon/k_BT = 0.5$. The figure compares results from the direct method for the excess chemical potential calculation for MSA (triangles), PY (squares), MS (rhombs), HNC (reversed triangles), and PLHNC (stars) closures with the compressibility route results for the PY closure (circles) and grand canonical Monte Carlo simulations (filled circles).

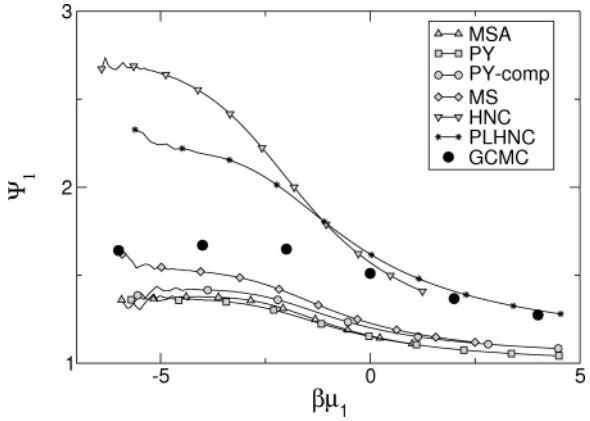

Figure 4. The ratio of the adsorbed fluid densities $\Psi_1 = \rho_1^{temp}(\beta\mu_1)/\rho_1^{nontemp}(\beta\mu_1)$ within system 1, for cases with and without a template component, as a function of the adsorbate chemical potential $\beta\mu_1$ as calculated for the MSA (triangles), PY (squares), MS (rhombs), HNC (reversed triangles), and PLHNC (stars) closures. Also shown are the results from the compressibility route with the PY closure (circles) and grand canonical Monte Carlo simulations (filled circles).

subspace method (MDIIS)[59] as well as their comparatively low overall porous material density (80% porosity).

In order to assess the effect of the template on adsorption, we introduce the parameter $\Psi_1 = \rho_1^{temp}(\beta\mu_1)/\rho_1^{nontemp}(\beta\mu_1)$ to compare the adsorbate density at a specified chemical potential in a templated system $\rho_1^{temp}(\beta\mu_1)$ to that in a nontemplated system $\rho_1^{nontemp}(\beta\mu_1)$ at the same matrix density. This parameter plotted as a function of chemical potential for system 1 is given in Figure 4. Both simulation and theory predict appreciable enhancement of adsorption due to the presence of the template. It is clear that one group of closures (MS, PY, PY-comp, and MSA) underestimates the extent of this effect, with the MS closure being slightly more realistic at lower chemical potentials. The HNC and PLHNC tend to overestimate this effect, particularly at lower chemical potentials. None of the closures provide quantitative agreement, but the decreasing trend with adsorbate density/chemical potential is qualitatively captured.

Convergence problems limit our study of adsorbed molecular species to the PY and MSA closures. In Figure 5, we compare adsorption isotherms from the PY method (both direct and

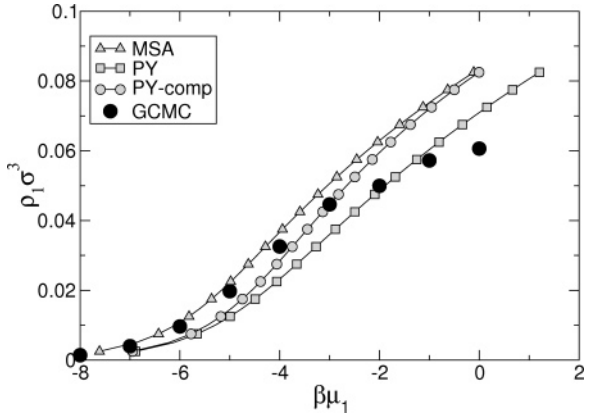

Figure 5. The adsorption isotherms (adsorbate density $\rho_1\sigma^3 = (N_1/V)\sigma^3$ as a function of the total adsorbate chemical potential $\beta\mu_1$) for system 2. The matrix density is $\rho_0\sigma^3 = 0.5$, the template density is $M_{0'}\rho_{0'}\sigma^3 = 0.3$, $M_{0'} = 3$, and the potential well depth is $\epsilon/k_BT = 0.5$. The figure compares results from the direct method for the excess chemical potential calculation for MSA (triangles) and PY (squares) closures with the compressibility route results for the PY closure (circles) and grand canonical Monte Carlo simulations (filled circles).

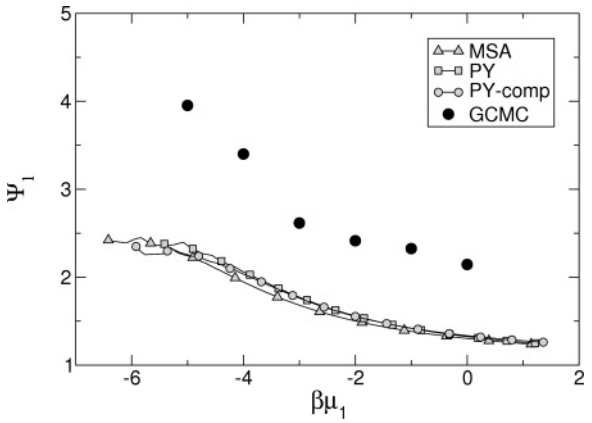

Figure 6. The ratio of the adsorbed fluid densities $\Psi_1 = \rho_1^{\text{temp}}(\beta\mu_1)/\rho_1^{\text{nontemp}}(\beta\mu_1)$ within system 2, for cases with and without a template component, as a function of the adsorbate chemical potential $\beta\mu_1$ as calculated for the MSA (triangles) and PY (squares) closures. Also shown are the results from the compressibility route with the PY closure (circles) and grand canonical Monte Carlo simulations (filled circles).

compressibility data), the MSA direct method, and the grand canonical computer simulations. All three methods show qualitative agreement with simulation, with the MSA method performing slightly better in the low-density regime. Given the results of the simple fluid system (Figure 2) and those of our previous work on hard-sphere systems, this agreement appears to result from some cancellation of certain errors. The computer simulation isotherm starts to show some signs of saturation at the values of chemical potential around −3. This is not captured in the theoretical predictions. The onset of this saturation for the theoretical isotherms is difficult to estimate as the calculations run into solution convergence problems before we reach the appropriate range of the chemical potential values. The effect of the template presence on adsorption characteristics of system 2 is shown in Figure 6. Again, the presence of the template component leads to the enhanced porosity, with the effect being stronger at low densities. This effect is also more pronounced compared to the simple fluid system. As in system 1, the MSA and PY closures underestimate the extent of the template effect and generate very similar results.

Results for system 3 are summarized in Figure 7. In particular, two sets of isotherms are shown. Black symbols correspond to

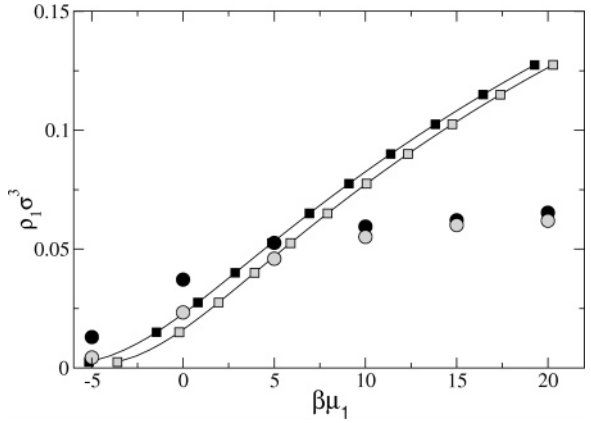

Figure 7. The adsorption isotherms (adsorbate density $\rho_1\sigma^3 = (N_1/V)\sigma^3$ as a function of the total adsorbate chemical potential $\beta\mu_1$) for system 3. The matrix density is $\rho_0\sigma^3 = 0.5$, the template density is $M_{0'}\rho_{0'}\sigma^3 = 0.3$, $M_{0'} = 3$, the mole fraction of functional monomers in the matrix component is $^1/_3$, and the potential well depth for the interaction between functional groups and functional monomers is $\epsilon/k_BT = 2.0$. The matrix is templated with AAB species. Black symbols are used for AAB adsorbate and gray symbols are used for ABA adsorbate. Squares connected with lines correspond to the theoretical predictions from the PY closure, whereas the simulations results are shown with larger, disconnected circles.

AAB fluid adsorbing in an AAB-templated matrix, whereas gray symbols correspond to ABA fluid adsorbing in the AAB-templated matrix. Lines connecting squares correspond to the PY approximation, and large, unconnected circles correspond to computer simulation. Several aspects are noteworthy here. First, the quality of the theoretical predictions is similar to that observed for the purely repulsive systems[50] and is clearly worse than that of systems 1 and 2. The theory underestimates the density of adsorbed fluid at low chemical potentials and overestimates this density at higher chemical potentials. This result is in line with our earlier observations for purely repulsive systems. Furthermore, the simulation results clearly exhibit adsorption saturation, which is not the case for the theoretical predictions. Similarly to system 2, the saturation region of adsorption isotherms could not be explored in full detail using the theoretical approach because of the convergence issues. Second, despite these quantitative differences, the theory is able to predict preferential adsorption of AAB species in the AAB-templated matrix, and the magnitude of this effect is broadly in line with that determined via simulation. In addition, the theory correctly predicts that the magnitude of this effect decreases with the increasing adsorbed fluid density, although this subtle observation is less evident from the figure. We thus present here the first molecular recognition effect predicted by integral equation theory.

7. Discussion

We present here a theoretical model of adsorption in a templated porous material that is based on the replica method and the RISM integral equation formalism. Our original work on this topic was limited to hard-sphere site−site interactions.[50] The focus of the present article is on systems with simple attractive interactions. The objective is to explore the scope and accuracy of direct methods for the confined fluid chemical potential in combination with a range of commonly used closures.

Several systems are considered. We begin with a simple fluid confined in a quenched matrix of simple particles, where all interactions are hard sphere and Lennard-Jones tail. The

quenched matrix is formed from an equilibrium mixture of matrix and template species, where the template species are identical to the adsorbate. Although none of the closure approximations we employ are quantitatively accurate over the entire isotherm, the MS and PY-comp closures produce reasonable agreement with computer simulation. (Interestingly, these two closures also provide the best prediction of the corresponding bulk system.)

The model is then extended to adsorbate and template species of rigid, three-site chains, where the site−site interactions are hard sphere and Lennard-Jones tail. Convergence problems for the numerical solution of the integral equations limit our consideration here to the MSA and PY closures. These approximations yield qualitatively accurate predictions and allow for assessment of the impact of templating on adsorption characteristics.

Finally, we examine a system with heterogeneous interactions. In particular, we impose that one of the three sites in the molecule (either a terminal or central one) can form attractive interactions with some of the matrix particles, imitating the functional associations found in real imprinted materials. All other site−site interactions are of the hard-sphere type. Again, only PY and MSA closures are accessible. Nonetheless, the theory is able to predict selective adsorption of a molecular species identical to the template in this case, the first observation (to our knowledge) of templated molecular recognition in a theoretical model. The molecular recognition effect is further confirmed by computer simulations. The theory, however, proves to be less accurate for absolute values of adsorption in systems with heterogeneous interactions.

The thermodynamic inconsistencies characteristic of the approximate theories of the liquid state are also present for fluids confined in templated materials. We show here for a given closure (PY), the direct method for the chemical potential of adsorbed fluid leads to a different adsorbed density than does the compressibility route. On the other hand, the direct chemical potential method offers a significantly more efficient numerical procedure, with comparable accuracy. In order to transform the theory from a qualitative to quantitative description, we suggest exploration of self-consistent closures.

Systems interacting via hard-core and attractive tail potentials are often well modeled by the mean spherical approximation together with the internal energy route toward the system free energy.[60] We note here that the MSA closure together with the direct chemical potential route performs no better than, and in some cases worse than, the other closure relations considered here. The PY closure is often employed together with integration of the isothermal compressibility to obtain the pressure (or via the Gibbs−Duhem relation, the chemical potential). While this approach has the undesirable feature of requiring correlation functions at all densities up to the density of interest, it does appear to fare better here compared to the PY closure and direct route toward the chemical potential for bulk and simple quenched−annealed systems. (For molecular systems, both PY-based approaches fare comparably.)

We consider here only cases where a single closure relation is used to solve all integral equations. In fact, eqs 2−4 (involving matrix and template species) are solved separately from eqs 5−8 (involving fluid species within a fixed matrix), so in principle each set could be solved within a different closure approximation. An interesting future direction would be to first optimize the accuracy of eqs 2−4, which are just those of a bulk mixture, and then test these best values of the matrix/template correlations functions with various closures for solving eqs 5−8. One could even determine the matrix/template correlation function by a very long canonical Monte Carlo simulation and then use the theoretical methods developed here to determine the subsequent adsorption isotherms. In this way, the accuracy of a given closure with respect to material structure and adsorbed fluid behavior could be distinguished.

The relatively modest magnitude of the molecular recognition effect in both theory and simulation results from the very simple molecular geometry and weak interaction energy. More realistic models would involve more complex molecular species with a number of heterogeneous interaction sites. Interaction energy strengths characteristic of electrostatic and hydrogen bond interactions should also be employed. The present work clearly reveals that in order to approach more realistic models, further research is needed toward thermodynamically self-consistent theoretical closure relations and more robust and efficient solution algorithms.

Acknowledgment. The authors wish to thank the National Science Foundation for financial support through Grant No. CTS-0337829 and the Engineering and Physical Sciences Research Council for financial support through Grant No. EP/D074762/01.

References and Notes

(1) Alexander, C.; Andersson, H. S.; Andersson, L. I.; Ansell, R. J.; Kirsch, N.; Nicholls, I. A.; O'Mahony, J.; Whitcombe, M. J. *J. Mol. Recognit.* **2006**, *19*, 106.
(2) Turiel, E.; Martin-Esteban, A. *Anal. Bioanal. Chem.* **2004**, *378*, 1876.
(3) Ye, L.; Haupt, K. *Anal. Bioanal. Chem.* **2004**, *378*, 1887.
(4) Davis, M. E.; Katz, A.; Ahmad, W. R. *Chem. Mater.* **1996**, *8*, 1820.
(5) Vlatakis, G.; Andersson, L. I.; Muller, R.; Mosbach, K. *Nature* **1993**, *361*, 645.
(6) Karim, K.; Breton, F.; Rouillon, R.; Piletska, E. V.; Guerreiro, A.; Chianella, I.; Piletsky, S. A. *Adv. Drug Delivery Rev.* **2005**, *57*, 1795.
(7) Chianella, I.; Lotierzo, M.; Piletsky, S. A.; Tothill, I. E.; Chen, B. N.; Karim, K.; Turner, A. P. F. *Anal. Chem.* **2002**, *74*, 1288.
(8) Chianella, I.; Karim, K.; Piletska, E. V.; Preston, C.; Piletsky, S. A. *Anal. Chim. Acta* **2006**, *559*, 73.
(9) Pavel, D.; Lagowski, J. *Polymer* **2005**, *46*, 7528.
(10) Monti, S.; Cappelli, C.; Bronco, S.; Giusti, P.; Ciardelli, G. *Biosens. Bioelectron.* **2006**, *22*, 153.
(11) Madden, W. G.; Glandt, E. D. *J. Stat. Phys.* **1988**, *51*, 537.
(12) Fanti, L. A.; Glandt, E. D.; Madden, W. G. *J. Chem. Phys.* **1990**, *93*, 5945.
(13) Macelroy, J. M. D.; Raghavan, K. *J. Chem. Phys.* **1990**, *93*, 2068.
(14) Given, J. A. *Phys. Rev. A* **1992**, *45*, 816.
(15) Madden, W. G. *J. Chem. Phys.* **1992**, *96*, 5422.
(16) Lomba, E.; Given, J. A.; Stell, G.; Weis, J. J.; Levesque, D. *Phys. Rev. E* **1993**, *48*, 233.
(17) Vega, C.; Kaminsky, R. D.; Monson, P. A. *J. Chem. Phys.* **1993**, *99*, 3003.
(18) Given, J. A.; Stell, G. R. *Physica A* **1994**, *209*, 495.
(19) Rosinberg, M. L.; Tarjus, G.; Stell, G. *J. Chem. Phys.* **1994**, *100*, 5172.
(20) Gordon, P. A.; Glandt, E. D. *J. Chem. Phys.* **1996**, *105*, 4257.
(21) Page, K. S.; Monson, P. A. *Phys. Rev. E* **1996**, *54*, 6557.
(22) Page, K. S.; Monson, P. A. *Phys. Rev. E* **1996**, *54*, R29.
(23) Kierlik, E.; Rosinberg, M. L.; Tarjus, G.; Monson, P. A. *J. Phys.: Condens. Matter* **1996**, *8*, 9621.
(24) Meroni, A.; Levesque, D.; Weis, J. J. *J. Chem. Phys.* **1996**, *105*, 1101.
(25) Pitard, E.; Rosinberg, M. L.; Tarjus, G. *Mol. Simul.* **1996**, *17*, 399.
(26) Trokhymchuk, A.; Pizio, O.; Holovko, M.; Sokolowski, S. *J. Phys. Chem.* **1996**, *100*, 17004.
(27) Pizio, O.; Sokolowski, S. *Phys. Rev. E* **1997**, *56*, R63.
(28) Pizio, O.; Trokhymchuk, A.; Henderson, D.; Labik, S. *J. Colloid Interface Sci.* **1997**, *191*, 86.
(29) Fernaud, M. J.; Lomba, E.; Lee, L. L. *J. Chem. Phys.* **1999**, *111*, 10275.
(30) Ilnytsky, J.; Patrykiejew, A.; Sokolowski, S.; Pizio, O. *J. Phys. Chem. B* **1999**, *103*, 868.
(31) Sarkisov, L.; Monson, P. A. *Phys. Rev. E* **2000**, *61*, 7231.
(32) Rzysko, W.; Sokolowski, S.; Pizio, O. *J. Chem. Phys.* **2002**, *116*, 4286.

(33) Fernaud, M. J.; Lomba, E.; Weis, J. J.; Levesque, D. *Mol. Phys.* **2003**, *101*, 1721.
(34) Pellicane, G.; Caccamo, C.; Wilson, D. S.; Lee, L. L. *Phys. Rev. E* **2004**, *69*, 10.
(35) Zhang, L. H.; Van, Tassel, P. R. *Mol. Phys.* **2000**, *98*, 1521.
(36) Zhang, L. H.; Van, Tassel, P. R. *J. Chem. Phys.* **2000**, *112*, 3006.
(37) Fernaud, M. J.; Lomba, E.; Weis, J. J. *Phys. Rev. E* **2001**, *6405*, 10.
(38) Kirkwood, J. G. *J. Chem. Phys.* **1935**, *3*, 300.
(39) Kirkwood, J. G. *Chem. Rev.* **1936**, *19*, 275.
(40) Morita, T. *Prog. Theor. Phys.* **1960**, *23*, 829.
(41) Morita, T.; Hiroike, K. *Prog. Theor. Phys.* **1960**, *23*, 1003.
(42) Lee, L. L. *J. Chem. Phys.* **1974**, *60*, 1197.
(43) Verlet, L.; Levesque, D. *Physica* **1962**, *28*, 1124.
(44) Kjellander, R.; Sarman, S. *J. Chem. Phys.* **1989**, *90*, 2768.
(45) Lee, L. L. *J. Chem. Phys.* **1992**, *97*, 8606.
(46) Kovalenko, A.; Hirata, F. *J. Chem. Phys.* **2001**, *115*, 8620.
(47) Kovalenko, A.; Hirata, F. *J. Chem. Phys.* **1999**, *110*, 10095.
(48) Kovalenko, A.; Hirata, F. *J. Phys. Chem. B* **1999**, *103*, 7942.
(49) Singer, S. J.; Chandler, D. *Mol. Phys.* **1985**, *55*, 621.
(50) Sarkisov, L.; Van, Tassel, P. R. *J. Chem. Phys.* **2005**, *123*, 10.
(51) Zhang, L. H.; Cheng, S. Y.; Van Tassel, P. R. *Phys. Rev. E* **2001**, *6404*, 4.
(52) Zhao, S. L.; Dong, W.; Liu, Q. H. *J. Chem. Phys.* **2006**, *125*, 16.
(53) Labik, S.; Malijevsky, A.; Vonka, P. *Mol. Phys.* **1985**, *56*, 709.
(54) Percus, J. K.; Yevick, G. J. *Phys. Rev.* **1958**, *110*, 1.
(55) Madden, W. G.; Rice, S. A. *J. Chem. Phys.* **1980**, *72*, 4208.
(56) Lebowitz, J. L.; Percus, J. K. *Phys. Rev.* **1966**, *144*, 251.
(57) Martynov, G. A.; Sarkisov, G. N. *Mol. Phys.* **1983**, *49*, 1495.
(58) Sarkisov, G. N. *Usp. Fiz. Nauk* **1999**, *169*, 625.
(59) Kovalenko, A.; Ten-No, S.; Hirata, F. *J. Comput. Chem.* **1999**, *20*, 928.
(60) Smith, W. R.; Henderson, D.; Tago, Y. *J. Chem. Phys.* **1977**, *67*, 5308.